UCRL-JC-121781
PREPRINT

Relaxation Spectra of Surface Waves

Daniel L. Marcus
Mark Sussman
Center for Computational Sciences & Engineering
P.O. Box 808, L-316
Lawrence Livermore National Laboratory
Livermore, CA 94551 U.S.A.

David Chambers
L-Division
P.O. Box 808, L-316
Lawrence Livermore National Laboratory
Livermore, CA 94551 U.S.A.

This paper was prepared for submittal to the
Forum on Advances in Numerical Modeling of Free Surface
and Interface Fluid Dynamics, 1995, San Francisco, CA
to be held November 12, 1995

August 1995

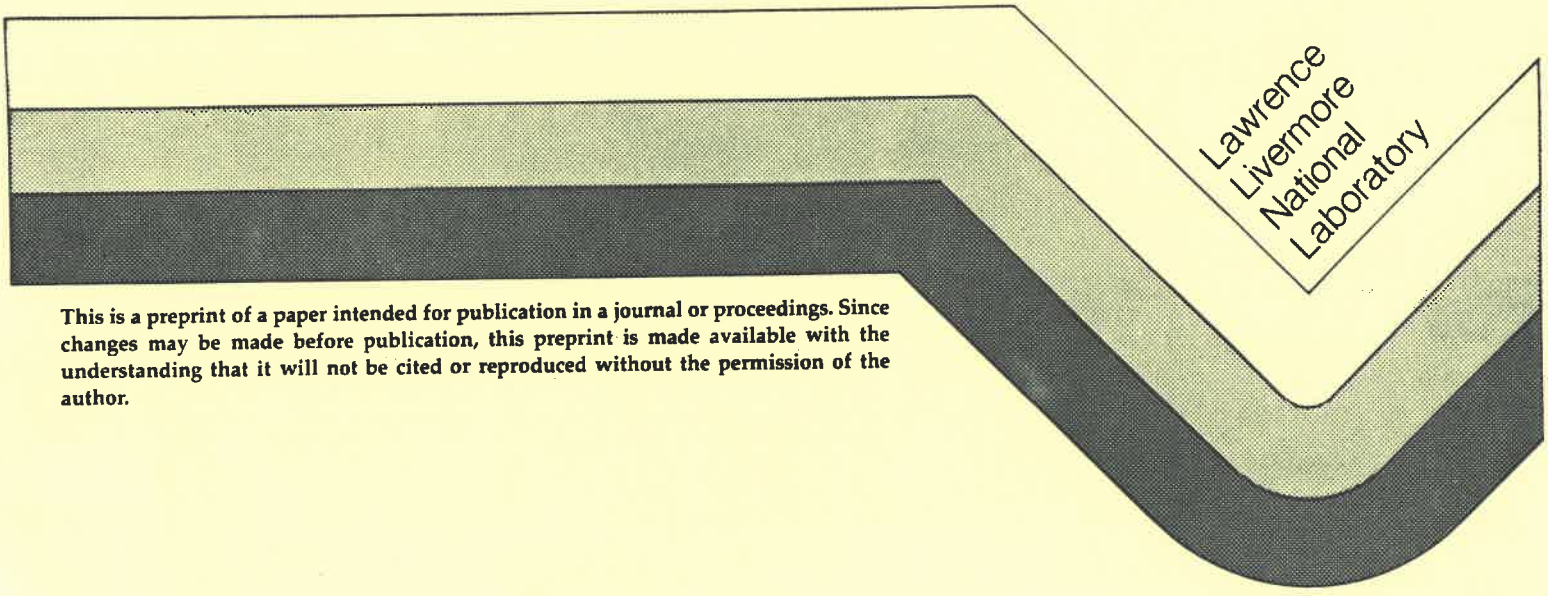

RELAXATION SPECTRA OF SURFACE WAVES

Daniel L. Marcus
Mark Sussman
Center for Computational Sciences and Engineering
Lawrence Livermore National Laboratory
Livermore, CA

David Chambers
L-Division
Lawrence Livermore National Laboratory
Livermore, CA

Abstract

A new method is described for computing free surface flows. The method allows for arbitrary wind profiles to be imposed above the surface as well as arbitrary subsurface current and density profiles. The method combines recent advances in projection methods for stratified flows with level set strategies for computing the motion of a distinguished interface. High resolution discretization schemes provide robust and accurate treatment of advection, even for singular initial data and in the limit of vanishing viscosity. The method is applied to the modulation of a nonlinear Stokes wave by wind applied at the surface. Speeds of 4,6, and 8 m/s relative to the rest frame are considered. The initial relaxation rate, β, is calculated. The phase and phase speeeds of the complex Fourier coefficient of the fundamental are found to increase with wind speed.

*This work was performed under the auspices of the U.S. Department of Energy by the Lawrence Livermore National Laboratory under contract W-7405-Eng-48 and under contract for the Office of the Secretary of Defense, C^3I. Support under contract W-7405-Eng-48 was provided by the Applied Mathematical Sciences Program of the Office of Scientific Computing at DOE.

Introduction

When an equilibrium spectrum of waves on the surface of the ocean is disturbed by a sudden change in wind speed, or when a wind-driven equilibrium spectrum evolves from a flat, undisturbed surface, the change in the spectrum can be modeled by a source term in the evolution equation for the wave action, $N(\mathbf{k}, \mathbf{x}, t)$:

$$\frac{\partial N}{\partial t} + \nabla_k N \cdot \frac{d\mathbf{k}}{dt} + \nabla_x N \cdot \frac{d\mathbf{x}}{dt} = S_w \tag{1}$$

Caponi et al. (1988) express the source term S_w as

$$S_w = \beta \frac{\omega'}{k} F(1 - |\frac{F}{F_{eq}}|^{\alpha}) \tag{2}$$

where $F(\mathbf{k}, \mathbf{x}, \mathbf{t})$ is the spectral density function, related to the wave action $N(\mathbf{k}, \mathbf{x}, \mathbf{t})$ by

$$N(\mathbf{k}, \mathbf{x}, t) = \frac{\omega'}{k} F(\mathbf{k}, \mathbf{x}, t) \tag{3}$$

The equilibrium spectrum F_{eq} is determined heuristically. The coefficient α can be 1 or 2 depending on whether the restoring force is taken to be quadratic or cubic, and ω' is the intrinsic frequency, given by:

$$\omega'^2 = gk(1 + Tk^3) \tag{4}$$

Here, T is the surface tension coefficient and $k = |\mathbf{k}|$.

There are a number of models available for the relaxation rate β, based on different sets of wave growth data collected in the laboratory and on the open ocean. Some models consider β to be an initial growth rate. The general trend is consistent with physical intuition – that for a given wind, β is an increasing function of wavenumber (i.e. shorter waves have shorter relaxation times). The values, however, are spread over an order of magnitude.

In this study, we calculate relaxation spectra directly using a high-resolution discretization scheme for the full Navier-Stokes equations together

with a level-set interface capturing strategy for the free surface. From the primitive variable calculations, we determine the time evolution of the spectrum of the surface elevation; from that, we extract the evolution of the power spectral density of individual wavenumbers. Where possible, we then determine $\beta(k)$ from the initial component growth rates.

We treat the free surface as an internal boundary in a multi-fluid domain and solve the full Navier-Stokes equations using a variable density projection method (Bell and Marcus, 1992). Use of higher-order, monotonicity-constrained discretizations for the nonlinear advective terms ensure that steep velocity and vorticity gradients are resolved without anomalous smearing or spurious oscillations.

The motion of the interface is captured using a level set procedure (Osher and Sethian, 1988), (Sussman et al., 1994). In this approach, the free surface is taken to be the zero level set of a smooth distance function advected by the underlying flow field. Density and viscosity fields on either side of the interface are reconstructed from this function at each time step. Since the free surface is a level set, topological changes (such as breaking waves) are handled naturally.

Physics local to the interface, such as surface tension, is calculated using the Continuum Surface Force (CSF) method of Brackbill et al. (1992). In this approach, the surface force is expressed as a force density proportional to the local curvature, acting throughout a transition region of finite thickness. As the thickness of this region approaches zero, the conventional surface force is recovered. Thus, the interfacial physics can be calculated on a finite-difference grid if the thickness of the interface is allowed to remain $O(\Delta h)$, where Δh is the mesh spacing. The use of higher-order advection schemes gaurentees that this region does not spread appreciably as the calculation evolves.

Numerical Formulation

In Sussman et al. (1994), an Eulerian scheme was described for computing incompressible two-fluid flow where the density ratio across the interface is large (e.g. air/water) and surface tension and viscous effects are included. We use a scheme similar to that described above except that it has been modified for ocean wave applications.

Equations of Motion; level set formulation

In the work of Osher and Sethian (1988), the zero level set ($\{(x,y)/\phi(x,y) = 0\}$) of a smooth function ϕ is used to represent a sharp interface between two fluids. ϕ is positive in one fluid and negative in the other. It was shown in Osher and Sethian (1988), (for motion by mean curvature) that the equation $\phi_t + \vec{u}\cdot\vec{\nabla}\phi$ accurately moves the zero level set according to the velocity field $\vec{u}$ even through the merging and breaking up of fluid mass; such as breaking waves.

There are many reasons to formulate the Navier-Stokes equations in the level set formulation. Computing spatial derivatives for ϕ, such as in the advection equation and for computing curvature, is more accurate than computing those values for a non-smooth function. Furthermore, we maintain the level set function as a smooth distance function allowing us to give the interface a thickness fixed in time. Large density jumps (such as air-water) and surface tension both depend on the level set function being a distance function.

We solve the following equations for incompressible flow including gravitational,viscous, and surface tension effects. The equations in dimensionless form are

$$H(\phi) \equiv \begin{cases} 1 & \text{if } \phi > 0 \\ 0 & \text{if } \phi < 0 \\ 1/2 & \text{if } \phi = 0 \end{cases} \tag{5}$$

$$\delta(\phi) = \partial H/\partial\phi \tag{6}$$

$$\kappa(\phi) = \vec{\nabla}\cdot\frac{\vec{\nabla}\phi}{|\vec{\nabla}\phi|} \tag{7}$$

$$\rho(\phi) = H(\phi) + (\rho_2/\rho_1)(1 - H(\phi)) \tag{8}$$

$$\mu(\phi) = H(\phi) + (\mu_2/\mu_1)(1 - H(\phi)) \tag{9}$$

$$\phi_t = -\vec{u}\cdot\vec{\nabla}\phi \tag{10}$$

$$\vec{\nabla}\cdot\vec{u} = 0 \tag{11}$$

and

$$\vec{u}_t = -\vec{u}\cdot\vec{\nabla}\vec{u} - \vec{\nabla}p/\rho + \frac{1}{Fr}\hat{y} + \frac{1}{R}\vec{\nabla}\cdot(2\mu D)/\rho + \frac{1}{W}\kappa(\phi)\vec{\nabla}H(\phi)/\rho \tag{12}$$

The dimensionless groups used are Reynolds number ($R = \frac{\rho_1 LU}{\mu_1}$), Froude number ($Fr = \frac{U^2}{gL}$), and Weber number ($W = \frac{\rho_1 LU^2}{\sigma}$).

We assume periodic boundary conditions on the left and right sides of the domain, and far field boundary conditions on the top and bottom.

Projection

In Bell and Marcus (1992), a variable density projection method was described, in which a vector decomposition to enforce the divergence-free condition was coupled with high order upwind differencing of the convective terms in order to handle high Reynolds number flow. Briefly, we may write eqn (12) as:

$$\vec{u}_t + \vec{\nabla} p/\rho = L(\vec{u}, \phi) \tag{13}$$

We use the fact that $\vec{u}_t$ is divergence free and hence for two-dimensional flow, we can write it as:

$$\vec{u}_t = \vec{\nabla} \times s_t$$

If we multiply both sides of eqn (13) by ρ and take the curl of both sides:

$$-\vec{\nabla} \rho \vec{\nabla} s_t = \vec{\nabla} \times L \tag{14}$$

The above equation eliminates pressure from eqn (12).

Validation

Numerous validation studies have been performed under a wide range of conditions, for both the variable density projection (Bell and Marcus, 1992), (Marcus and Bell, 1994), and the level set approach (Sussman et al., 1994). In order to demonstrate the performance of the method for the class of problems considered in this study, we examine two cases. The first of these compares the numerical results with a linear model for the viscous attenuation of standing waves (Lamb, 1932). This problem was also used as a

validation by Dommermuth (1993). The surface elevation, $\eta(x,t)$, is given by

$$\eta = a_0 cos(kx) cos(\omega t) e^{-2\nu k^2 t} + O(\nu) \tag{15}$$

where ω^2 = k g *tanh* (k H). For $\nu^{-1} = 500$ and 1000 on a $100x100$ grid, the mean peak-to-peak errors in the amplitude were 1.6% and 0.9%, respectively. Figure 1 shows the analytical and computed solutions for the $\nu^{-1} = 1000$ case. In Figure 2, we plot the error as a function of Reynolds number. The results are consistent with the $O(\nu)$ error in the Lamb approximation.

Using a procedure due to Rienecker and Fenton (1981), we calculated the Fourier coefficients to an approximation of a steady Stokes wave. The code was initialized with that profile and the calculation performed in the wave frame, in the absence of viscosity or surface tension. (The expectation was, of course, that the profile would remain stationary). Figure 3 shows the time evolution of the surface elevation out to a dimensionless time $t = 20$. There has been a very slight phase shift, but its maginitude is negligible over the duration of interest.

Results

We begin with the Stokes wave described in the previous section and modulate it by imposing a steady wind profile in the air above it. The wind profile is given by

$$u(x,y;y>\eta) = U_0 tanh(\frac{y-\eta(x)}{\delta}) cos\phi \tag{16}$$

$$v(x,y;y>\eta) = -U_0 tanh(\frac{y-\eta(x)}{\delta}) sin\phi \tag{17}$$

where U_0 is the free-stream wind speed, $\eta(x)$ is the location of the surface, δ is of the order of the mesh spacing, and $\phi = tan^{-1}(\frac{\eta}{x})$. The profile is transitioned to a purely horizontal wind via a cubic spline interpolation.

Three different speeds are considered: $U_0 = (4, 6, 8)$ m/s (relative to the stationary frame). The domain is 10 m long and 5 m wide. Far field boundary conditions are imposed at top and bottom; the domain is periodic in x.

Figures 4-6 show the time evolution of the surface for the three cases. There is a discernible phase shift that becomes more pronounced as the wind speed is increased. Figure 7 is a plot of the phase of the complex Fourier coefficient of the fundamental as a function of time. The phase history is quadratic in time. A second-order polynomial was fit to each phase, then the derivative taken analytically to obtain a time history of the phase speed deviation (Figure 8). The solid lines are for the 4 m/s wind, the dashed line for the 6 m/s wind, and the dashed-dot lines for the 8 m/s wind. The corresponding accelerations are 9.08e-3 m/s^2 for 4 m/s wind, 1.04e-2 m/s^2 for 6 m/s wind, and 1.18e-2 m/s^2 for 8 m/s wind. Thus the phases, phase speeds, and accelerations all increase with wind speed.

In Figure 9, we plot the power spectral density of the fundamental mode as a function of time for the three cases. Superimposed on the wind-induced growth is a "sloshing" mode whose frequency corresponds to that of a deep-water gravity wave. The results at first appear counterintuitive; the wind suppresses the growth of the fundamental mode. But examination of the time histories of higher modes (Figures 10-14) reveals that eventually the more strongly forced higher modes overtake and surpass the weaker ones.

Figure 15 shows approximations of the relaxation rate $\beta(k)$ for the three wind speeds. The results were obtained by a straight-line fit through the first few points of a semi-log representation of the data. The slope then corresponds to a leading-order estimate of the relaxation rate. The trend is consistent with expectation; β is an increasing function of both wind speed and wavenumber. The influence of the wind is also more pronounced at higher wavenumbers.

Conclusions, Speculations, Ongoing and Future Work

We have demonstrated a potentially powerful strategy for studying the spectral evolution of wind-driven surface waves via numerical solution of the full Navier-Stokes equations. Our observation have been that the spectral results are very sensitive to the modeling of the surface wind profile. Further

studies are being carried out to better understand this sensitivity. The relaxation rate, β, is a complicated function of wavenumber, wind speed, and time; current models which use β as a leading order term are probably inadequate for fully characterizing relaxation phenomena. Calculating complete transitions between equilibrium spectra is computationally very taxing as it takes a long time for a new equilibrium state to become manifest. Complete characterizations of such transitions for wind-modulated waves will be the scope of a future paper. Other near-term plans for this work include a rigorous resolution study to further validate the technique described in this paper, dialogue with experimentalists on wind-modulation of surface waves, computational study of Benjamin-Feir instabilities, and detailed investigation of pre-and post-breaking spectra.

References

[1] J. B. Bell and D. L. Marcus, 1992, "A second-order projection method for variable-density flow," *J, Comp. Phys.*, **101**, 334.

[2] J. Brackbill, D. Kothe, and C. Zemach, 1992, "A continuum method for modeling surface tension," *J, Comp. Phys.*, **100**, 335.

[3] E.A. Caponi, D.R. Crawford, H.C. Yuen, and P.G. Saffman, 1988, "Modulation of radar backscatter from the ocean by a variable surface current," *J. Geophys. Res.*, **93**, C10, 12,249-12,263.

[4] D. G. Dommermuth, 1993, "The laminar interactions of a pair of vortex tubes with a free surface," *J. Fluid Mech.*, **246**, 91-115.

[5] H. Lamb, 1932, *Hydrodynamics*, Dover.

[6] D. L. Marcus and J. B. Bell, 1994, "Numerical simulation of a viscous vortex ring interaction with a density interface," *Phys. Fluids* **6**(4), 1505.

[7] S. Osher, J. Sethian, 1988, "Fronts propagating with curvature dependent speeds: algorithms based on Hamilton-Jacobi formulations," *J, Comp. Phys.*, **79**, 128.

[8] M. Rienecker and J. Fenton, 1981, "A Fourier approximation method for steady water waves," *J. Fluid Mech.*, **104**, 119.

[9] M. Sussman, P. Smereka, S. Osher, 1994, "A level set approach for computing solutions to incompressible, two-phase flow," *J, Comp. Phys.*, **114**, 146.

List of Figures

Figure 13. $\Psi_5(t)$, U = (4,6,8) m/s.

Figure 14. $\Psi_6(t)$, U = (4,6,8) m/s.

Figure 15. $\beta(k), k \in [3,6]$ U = (4,6,8) m/s.

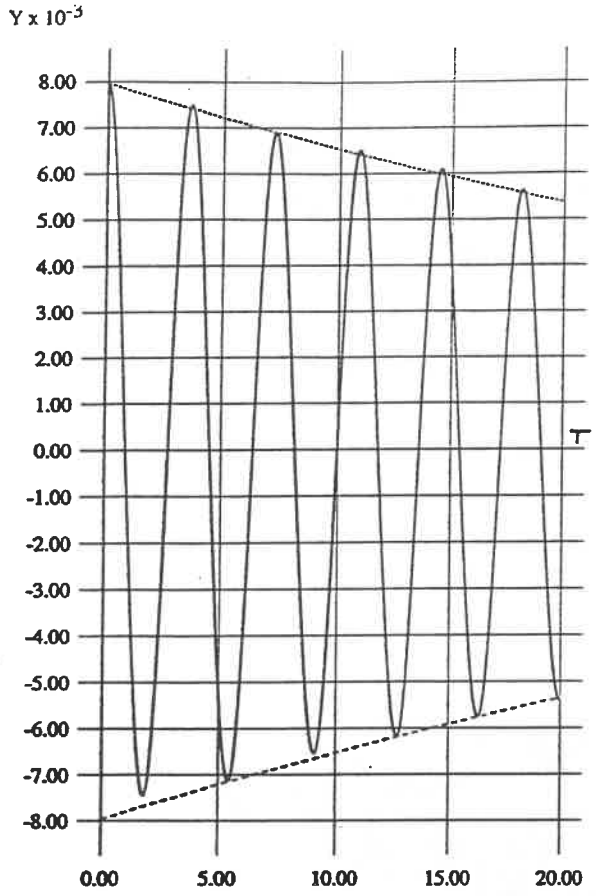

Figure 1

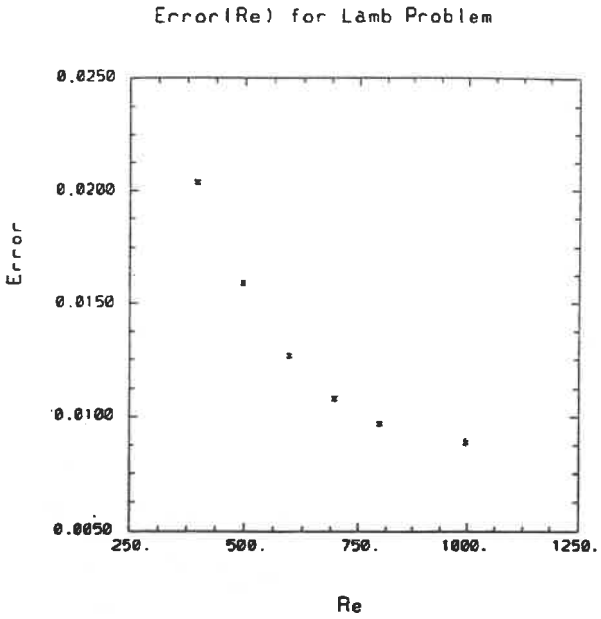

Figure 2

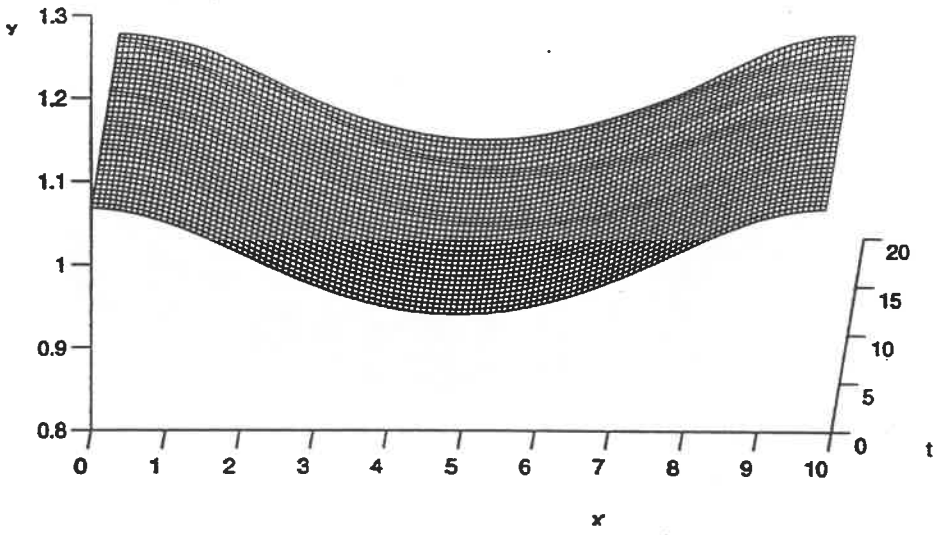

Figure 3

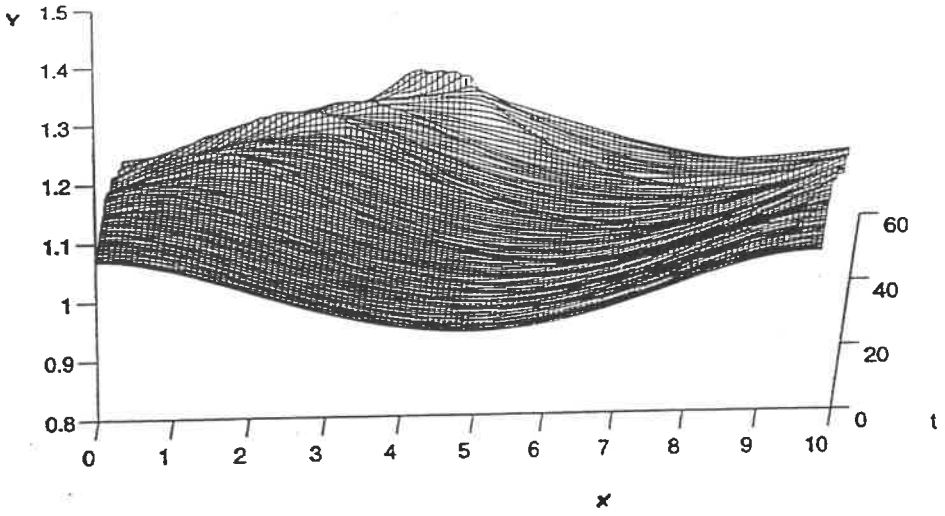

Figure 4

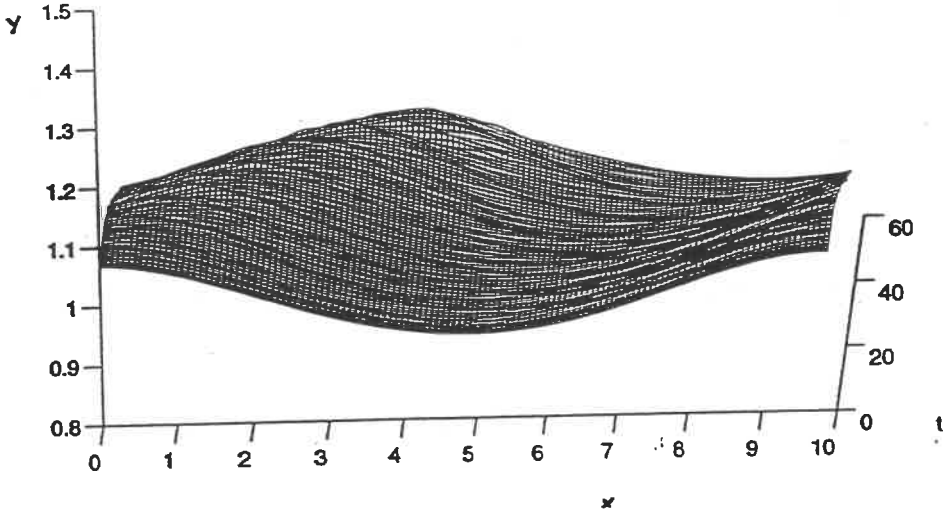

Figure 5

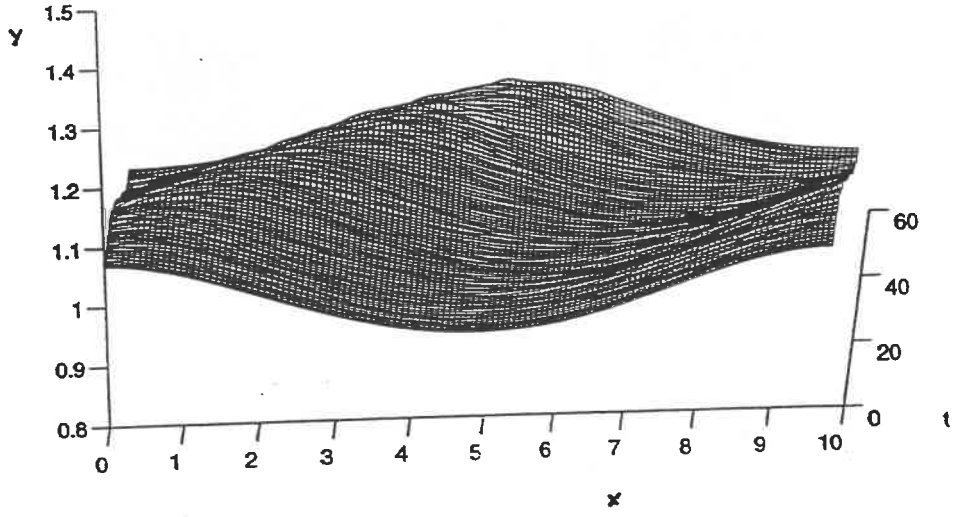

Figure 6.

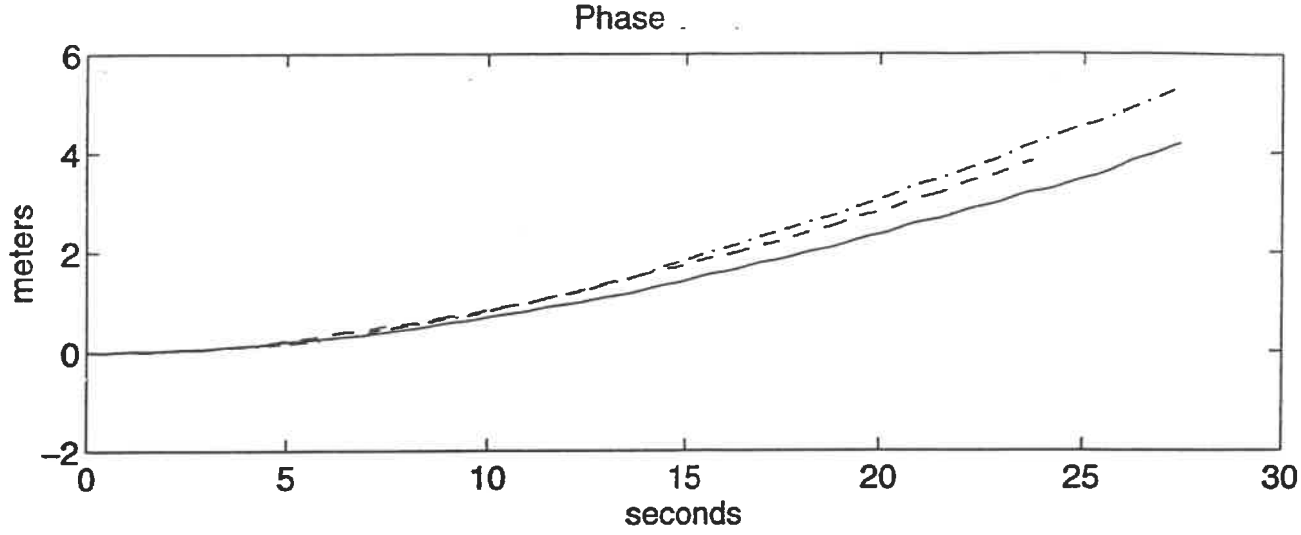

Figure 7

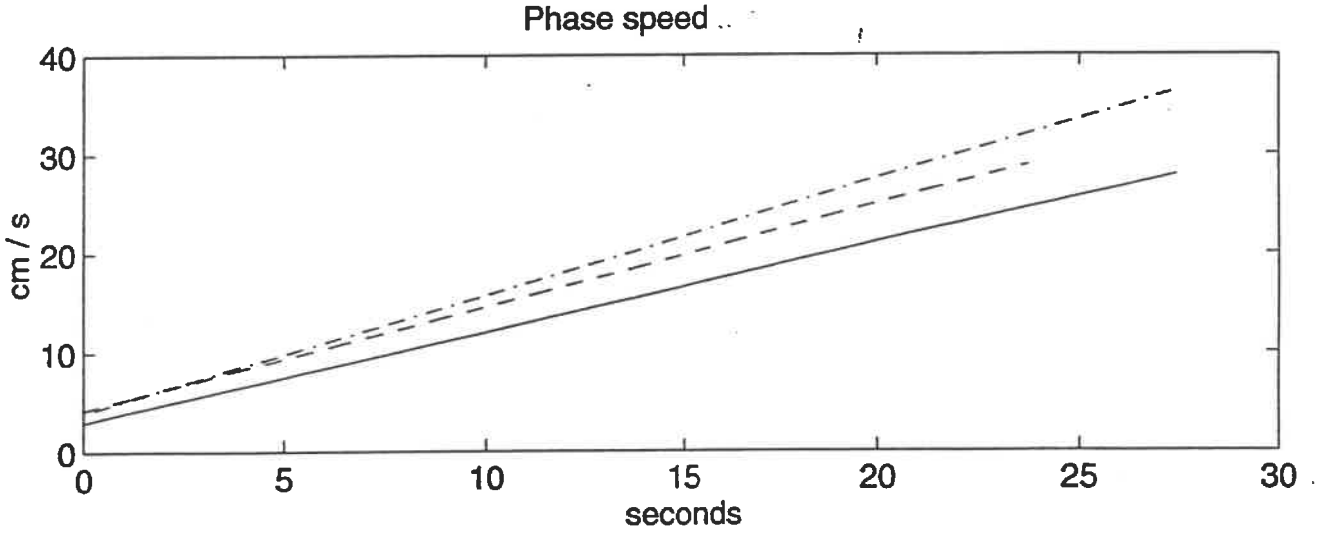

Figure 8

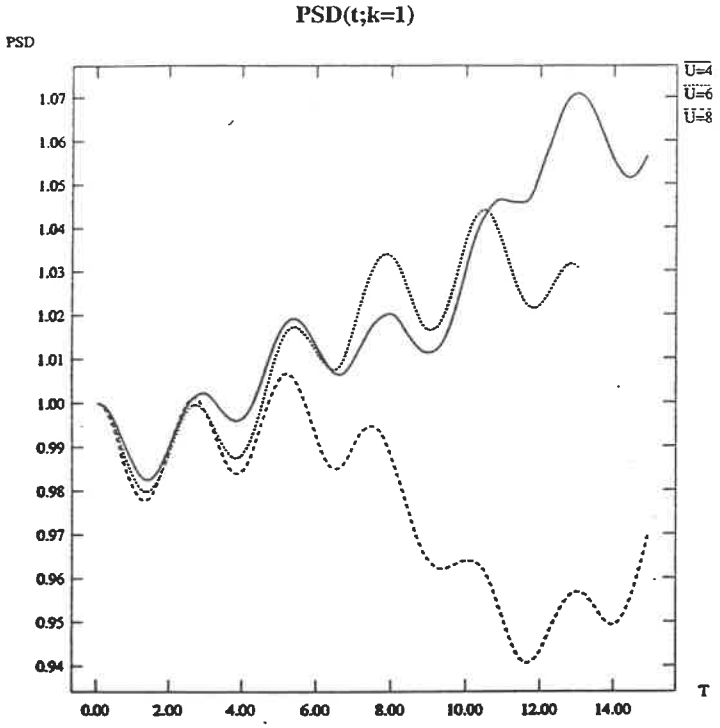

Figure 9.

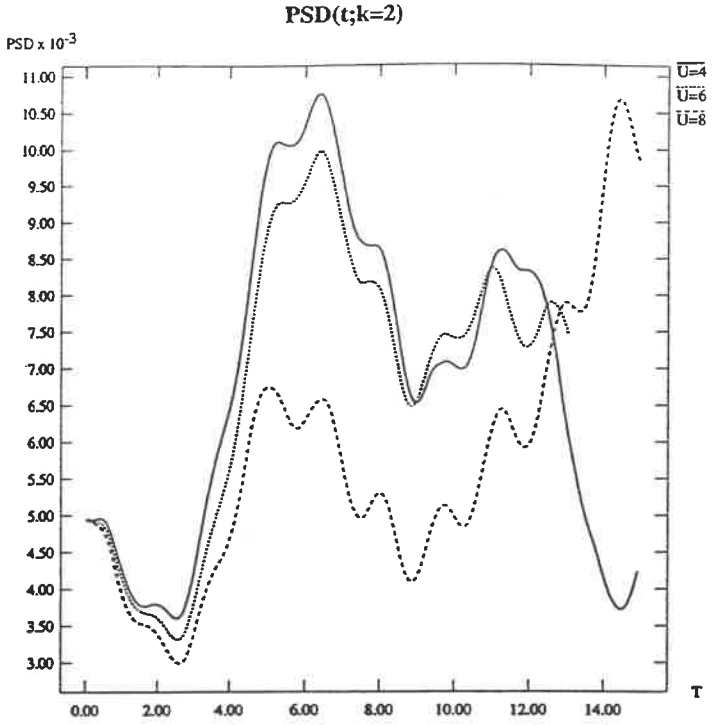

Figure 10.

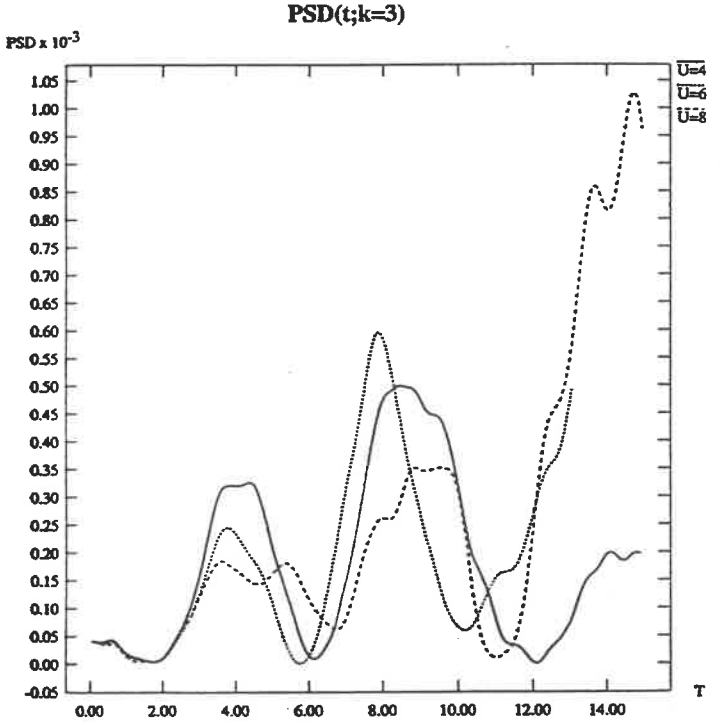

Figure 11.

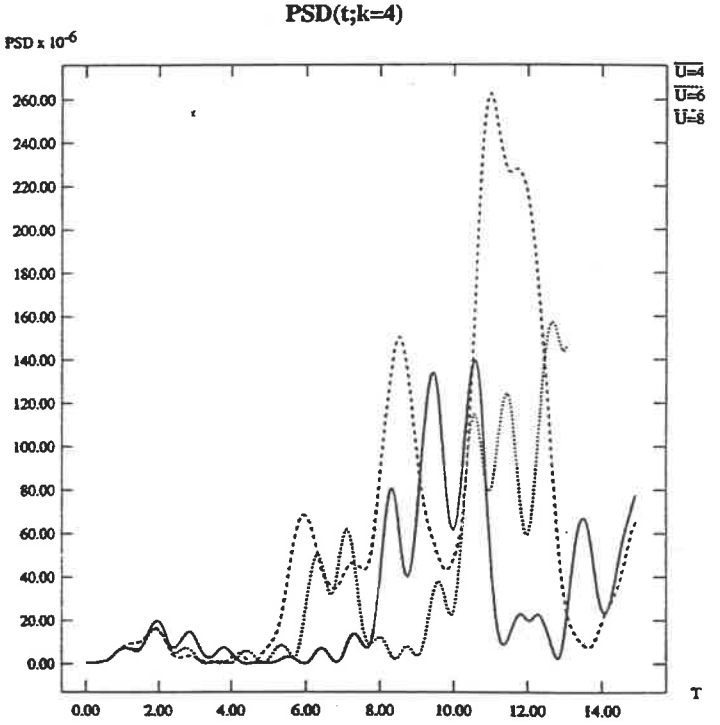

Figure 12

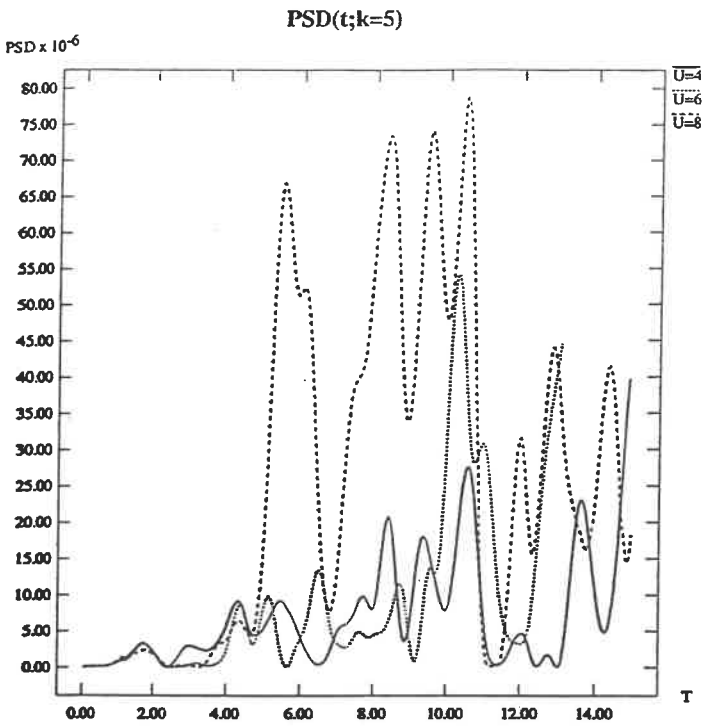

Figure 13

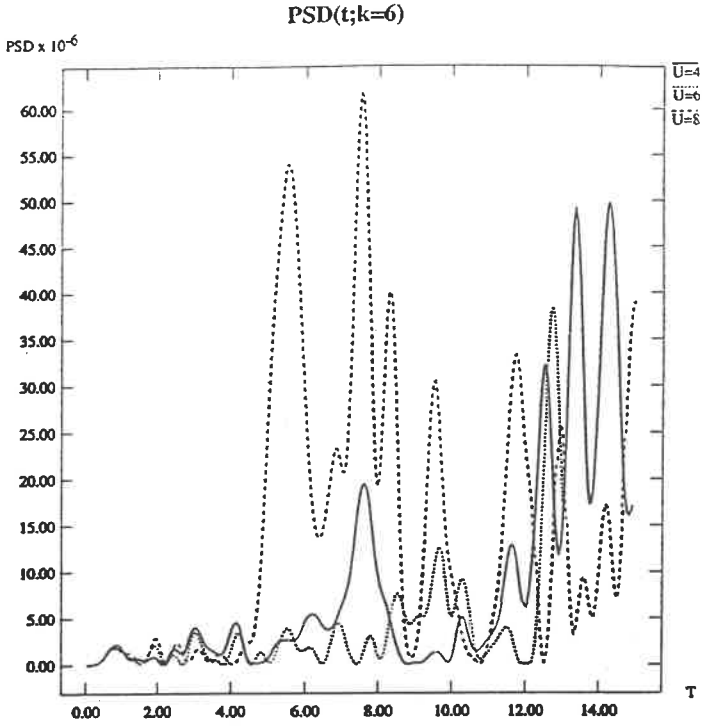

Figure 14

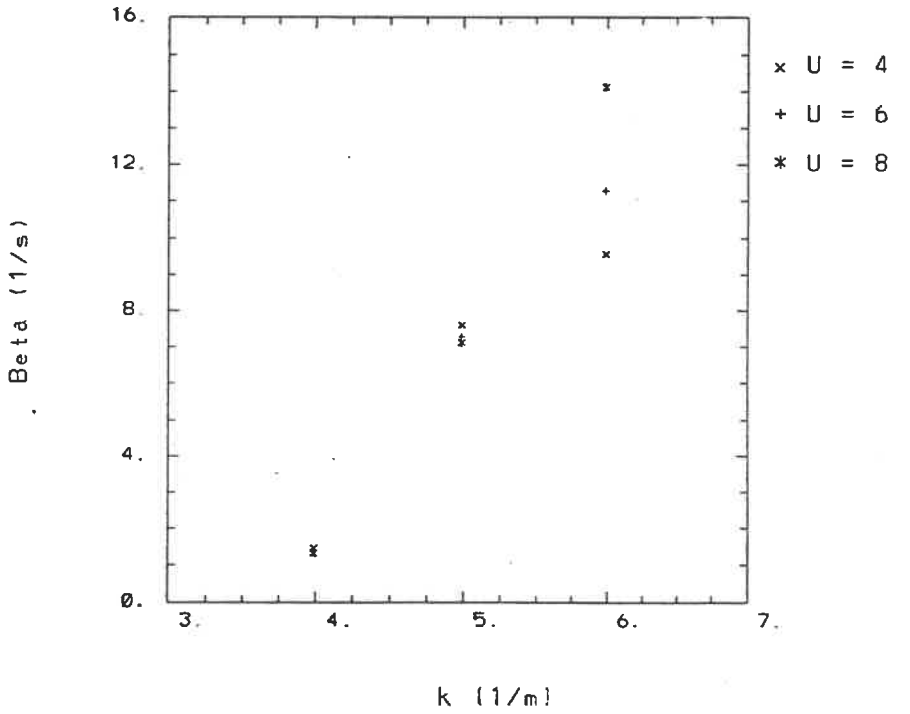

Figure 15

Technical Information Department · Lawrence Livermore National Laboratory
University of California · Livermore, California 94551